AD-A160 186 POPULATION INVERSION AND GAIN MEASUREMENTS FOR X-RAY 1/1
LASER DEVELOPMENT IN (U) PRINCETON UNIV N J PLASMA
PHYSICS LAB S SUCKEWER 20 MAR 85 AFOSR-TR-85-0809
UNCLASSIFIED AFOSR-84-0025 F/G 20/5 NL

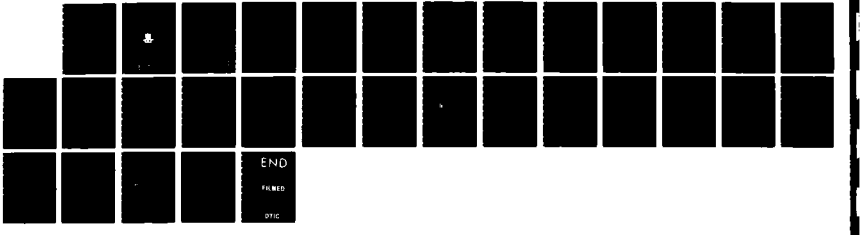

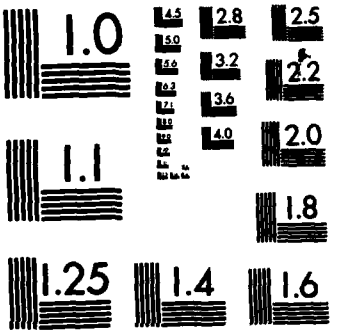

AFOSR-TR- 85-0809

(2)

REPORT ON PROGRESS ON POPULATION INVERSION AND GAIN MEASUREMENTS FOR X-RAY LASER DEVELOPMENT IN MAGNETICALLY CONFINED PLASMA COLUMN IN FY 84

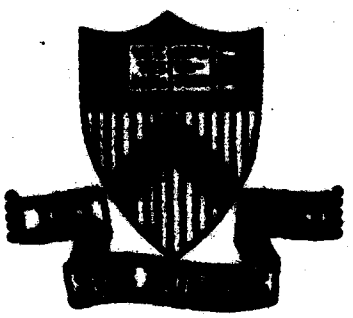

SUBMITTED TO

AIR FORCE OFFICE OF SCIENTIFIC RESEARCH

BY

PRINCETON UNIVERSITY PLASMA PHYSICS LABORATORY

Princeton, New Jersey 08544

REPORT ON PROGRESS ON POPULATION INVERSION AND GAIN MEASUREMENTS FOR X-RAY LASER DEVELOPMENT IN MAGNETICALLY CONFINED PLASMA COLUMN IN FY 84

SUBMITTED TO

AIR FORCE OFFICE OF SCIENTIFIC RESEARCH

BY

PRINCETON UNIVERSITY PLASMA PHYSICS LABORATORY

Princeton, New Jersey 08544

SECURITY CLASSIFICATION OF THIS PAGE

REPORT DOCUMENTATION PAGE

1a. REPORT SECURITY CLASSIFICATION: Unclassified	1b. RESTRICTIVE MARKINGS
2a. SECURITY CLASSIFICATION AUTHORITY	3. DISTRIBUTION/AVAILABILITY OF REPORT: Approved for public release; Distribution unlimited
2b. DECLASSIFICATION/DOWNGRADING SCHEDULE	
4. PERFORMING ORGANIZATION REPORT NUMBER(S): ~~AFOSR-84-0025~~	5. MONITORING ORGANIZATION REPORT NUMBER(S): ~~N/A~~ AFOSR-TR- 85-0809
6a. NAME OF PERFORMING ORGANIZATION: Princeton University Plasma Physics Lab. / 6b. OFFICE SYMBOL (If applicable)	7a. NAME OF MONITORING ORGANIZATION: AFOSR/NP
6c. ADDRESS (City, State and ZIP Code): Princeton, NJ 08544	7b. ADDRESS (City, State and ZIP Code): Building 410 Bolling AFB, DC 20332-6448
8a. NAME OF FUNDING/SPONSORING ORGANIZATION: AFOSR / 8b. OFFICE SYMBOL (If applicable): NP	9. PROCUREMENT INSTRUMENT IDENTIFICATION NUMBER: ~~AFOSR-84-0114~~ AFOSR-84-0025
8c. ADDRESS (City, State and ZIP Code): Building 410 Bolling AFB, DC 20332-6448	10. SOURCE OF FUNDING NOS. — PROGRAM ELEMENT NO.: 61102F / PROJECT NO.: 2301 / TASK NO.: A8 / WORK UNIT NO.:
11. TITLE (Include Security Classification): POPULATION INVERSION AND GAIN MEASUREMENTS FOR X-RAY	
12. PERSONAL AUTHOR(S): Dr. Szymon Suckewer	
13a. TYPE OF REPORT: Annual / 13b. TIME COVERED: FROM 11/83 TO 10/84	14. DATE OF REPORT (Yr., Mo., Day): March 20, 1985 / 15. PAGE COUNT: 30
16. SUPPLEMENTARY NOTATION: title cont.: LASER DEVELOPMENT IN MAGNETICALLY CONFINED PLASMA COLUMN IN FY 84	

17. COSATI CODES			18. SUBJECT TERMS (Continue on reverse if necessary and identify by block number)
FIELD	GROUP	SUB. GR.	X-Ray Laser; Carbon (6+) XUV Laser.

19. ABSTRACT (Continue on reverse if necessary and identify by block number)

This report covers the period November 1, 1983 through October, 31, 1984 (FY 84). During this period we have investigated X-ray laser development in magnetically confined plasmas, as well as in expanding recombining plasma columns using time resolved soft X-ray monochromators. Experiments with both solid and gas targets resulted in gain measurements for hydrogen-like (CVI) ions and population inversion measurements for lithium-like (NeVIII) ions. Our most recent results, involving carbon disc targets in a 90 kGauss field with a 300 Joule CO_2 laser pulse, in which a one-pass gain of $k\ell$ 6.5 (enhancement of stimulated emission over spontaneous emission about 100) was obtained for CVI 182Å are presented. Results of a gain $k\ell = 3.0$ ($k \approx 7.5$ /cm) for thick carbon fiber targets are also presented. Population inversions of NeVIII ions as a function of initial gas pressure are also discussed, as well as an overview of the instrumentation, experimental setup, and target configurations used. Keywords:

20. DISTRIBUTION/AVAILABILITY OF ABSTRACT	21. ABSTRACT SECURITY CLASSIFICATION
UNCLASSIFIED/UNLIMITED ☒ SAME AS RPT. ☒ OTIC USERS ☐	Unclassified
22a. NAME OF RESPONSIBLE INDIVIDUAL: ~~Dr. Barker~~ ~~Szymon Suckewer~~ S. Suckewer	22b. TELEPHONE NUMBER (Include Area Code): 202/767-~~4908~~ 4908 / 22c. OFFICE SYMBOL: NP

DD FORM 1473, 83 APR EDITION OF 1 JAN 73 IS OBSOLETE.

Carbon Dioxide laser

TABLE OF CONTENTS

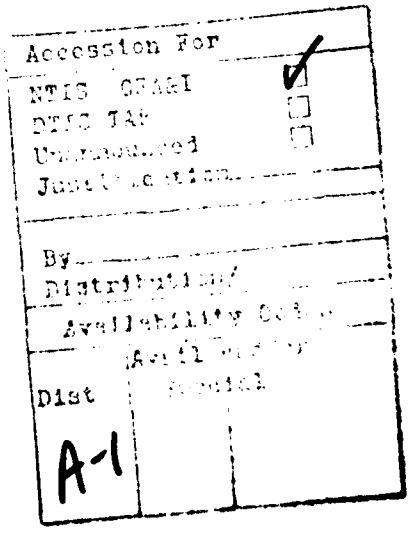

REPORT ON PROGRESS ON

THE X-RAY LASER DEVELOPMENT IN PPPL IN FY 1984

1.0 SUMMARY

This report covers the period November 1, 1983 through October 31, 1984 (FY 84). During this period we have investigated x-ray laser development in magnetically confined plasmas, as well as in expanding recombining plasma columns using time resolved soft x-ray monochromators. Experiments with both solid and gas targets resulted in gain measurements for hydrogen-like CVI ions and population inversion measurements for lithium-like NeVIII ions. Our most recent results, involving carbon disc targets in a 90 kGauss field, with a 300 Joule CO_2 laser pulse, in which a one-pass gain of $k\ell \approx 6.5$ (enhancement of stimulated emission over spontaneous emission ~ 100) was obtained for CVI 182 Å are presented. Results of a gain $k\ell = 3.0$ ($k \approx 7.5$ cm^{-1}) for thick carbon fiber targets are also presented. Population inversions of NeVIII ions as a function of initial gas pressure are also discussed, as well as an overview of the instrumentation, experimental setup, and target configurations used.

2.0 GENERAL

Of the many possible approaches including recombination, line coincidence, photo-pumping, and multi-photon ionization schemes, to the development of an x-ray laser, PPPL has chosen the recombination scheme as the most promising for a relatively small experiment. For this approach to be successful, the requirements of fast plasma cooling, and simultaneously that there be uniform plasma conditions in the direction of expected lasing action, must be met. To achieve these requirements, the PPPL approach is to create a

plasma that is confined in a strong magnetic field and is rapidly cooled by radiation losses. We have shown experimentally that radiation cooling of a magnetically confined plasma column can be more effective than adiabatic cooling of a freely expanding plasma.

The plasma is created by focusing a 1 kiloJoule CO_2 laser pulse onto a solid or gas target. The plasma is confined to an axial column of relatively large length to radius ratio ($\ell/r > 100$) by the solenoidal magnetic field, thereby preventing a rapid decrease in the electron density. Because the spectral line radiation losses are proportional to Z^4, and three body recombination is proportional to n_e^2, such cooling can produce very rapid recombination in a plasma with high enough Z and n_e.

Comparison between the time integrated spectra in the axial direction, which is along the expected lasing line, and the transverse direction, which is perpendicular to the line of lasing action, indicates an enhancement of the CVI 182 Å line, and also population inversion for the Li-like CIV, OVI, FVII and NeVIII ions. Time evolution measurements along the axial and transverse directions are presented which show gain at the CVI 182 Å line.

Additional topics discussed in this report include the current experimental setup, the results obtained with various targets used during the current report period, and the experimental instrumentation used. A conclusion highlighting the most significant results obtained during the report period completes the report.

3.0 EXPERIMENTAL ARRANGEMENT AND INSTRUMENTATION

The experimental setup is shown schematically in Fig. 1. On the left is a 1 kiloJoule 10-20 GWatt Lumonics CO_2 TEA laser. The output of the laser, which is approximately a 70 ns FWHM pulse at 10.6 microns is focused onto the

target using a system of focusing mirrors while a small portion of the laser pulse is deflected to the Laser Beam Detector to provide a means for the data acquisition system to monitor the intensity and the time waveform of the laser pulse. The focusing mirror and the other portions of the optics are contained within the vacuum system. The target area is enclosed within a vacuum tube which itself is enclosed within a solenoidal magnet that can be pulsed to provide a peak magnetic field intensity of up to 90 kiloGauss. Various spectrometers and monochromators make up the remainder of the optical system.

The plasma emission in the axial direction is measured by an XUV grazing incidence monochromator equipped with a 16 stage electron multiplier, and emission in the transverse direction is measured by an XUV grazing incidence duochromator equipped with two channel electron multipliers. The rise time of the axial instrument is $\Delta t \approx 20$ nsec and approximately 10 nsec for the transverse one. Both instruments operate in the spectral range 10-350 Å. A streak camera is used to record the shape of the plasma in the visible region. An NaCℓ lens, which had been used for CO_2 laser focusing, has been replaced by a spherical copper focusing mirror with a 3 meter focal length. The laser beam is focused to ~ 200 micron spot resulting in a maximum density of 10^{13} W/cm^2.

The maximum enhancement, however, was measured for a laser energy ≈ 0.3 kJoule, power density ≈ 5 x 10^{12} W/cm^2 and pulse duration of FWHM ≈ 75 nsec.

3.1 TARGETS

The target arrangements were grouped into four categories: gas targets, carbon blades, carbon fibers, and carbon discs with and without aluminum blades. Typical target assemblies are shown in Fig. 2. The gas targets

(Fig. 2a), in which CO_2, O_2, and Ne were used, provided us with a longer and more uniform plasma column than the solid targets, but it was difficult to maintain optimum gas pressure within the vacuum chamber. After the gas puffing experiments, experimentation was concentrated on the solid targets. The solid targets were expected to enable us to obtain an electron density close to the critical density for the CO_2 laser wavelength of 10.6 microns, approximately $10^{19}cm^{-3}$. A series of experiments was conducted using aluminum coated carbon thick fibers (see Fig. 2c), 20-150 microns in diameter, supported on a pair of strands from spider webs or on carbon filaments. The spider web material offered the advantage of being very thin, and also relatively strong. The carbon fiber target was aligned axially in the target area, but had the disadvantage of being difficult to align in precisely the same spot from shot to shot, and also requiring replacement with a new target after each shot. Results with the carbon fibers were encouraging in that a maximum gain-length product of $k\ell \approx 3.0$ ($k \approx 7.5\ cm^{-1}$) at 182 Å was observed. The best results (enhancement ≈ 100, gain $k\ell \approx 6.5$), however, were obtained using the carbon disc with a horizontal slot. These results were preceded by experiments with a C-disc with a 1.0 to 1.5 mm hole through the center. In each case the CO_2 laser was focused on the edge of the hole. The carbon disc target was masked to enable the axial and transverse spectrometers to observe only the off axis region of the plasma. Figures 3a and 3b show two carbon discs, 2 mm thick. Each has a horizontal slot 0.8 mm x 4 mm located 1.5 mm above the center of the disc. The disc in Fig. 1b has a thin, 2 cm long carbon blade attached with the blade edge ~ 0.5 mm to the left of the central axis. Each disc was mounted in the vacuum chamber inside the magnet, with the normal to the surface colinear with the axis of the CO_2 laser beam. A mask with a slot (0.8 mm wide, and 2 cm long) parallel to the plasma column

limited the view of the transverse spectrometer to the off axis region at the same height as the slot in the disc. A grazing incidence mirror focused light from the center of the slot in the disc to the axial XUV monochromator.

3.2 CALIBRATION

The principal instrumentation used in the experiment is a soft X-ray (XUV) grazing incidence duochromator monitoring emission in the transverse direction from the target and an XUV monochromator-spectrometer observing in the axial direction. These instruments were carefully calibrated using several different techniques. The emission in the axial and transverse directions was simultaneously observed by two absolute intensity calibrated air monochromators using beam splitters so that each pair of XUV and air instruments observed practically the same region of the plasma. In this way, it was possible to use the branching ratio method to provide an in-situ absolute intensity calibration for the XUV instruments using both the laser produced plasma and independently, a high voltage vacuum spark specially built for calibration purposes.

The relative sensitivity of the axial and transverse instruments was obtained for the CVI 182 Å and CVI 33.7 Å lines by viewing the plasma created by the interaction of the CO_2 laser with a 70-300 μ diameter vertical fiber. This last method is considered more reliable than the branching ratio method for comparison of the sensitivity of the axial and transverse monochromators for use with laser created plasmas.

4.0 TECHNIQUES OF MEASUREMENT OF ENHANCEMENT

The enhancement (E) of stimulated emission over spontaneous emission of the CVI 182 Å line was measured in two ways and the consistency of enhancement (gain) was checked with the relative population of level n = 3 obtained from measurements of intensities in the axial and transverse directions. The first method was based on the comparison of the ratio of intensities of the CVI 182 Å line recorded simultaneously by axial and transverse XUV instruments (first laser shot) with the ratio of intensities of the CVI 135 Å (4 → 2 transition) also recorded simultaneously by axial and transverse XUV instruments (second laser shot) as follows:

$$E = \frac{I(182)_{axial}}{I(182)_{transv.}} \Big/ \frac{I(135)_{axial}}{I(135)_{transv.}} \qquad (1)$$

In Eq. (1), $I(\lambda)$ is the intensity of a line of wavelength λ integrated over the spectral profile and over length. The subscripts "axial" and "transv." refer to the direction of emission. The CVI 135 Å line was chosen for such a comparison because the lower and upper energy levels are close to that of the 182 Å line. One channel of the transverse duochromator recorded the CVI 33.7 Å line (2 → 1 transition) to monitor the reproducibility of CVI emission in the discharges. The contribution of the fourth order of the 33.7 Å line to the 135 Å line was subtracted. The transverse intensities of the 182 Å and 135 Å lines compared to the 33.7 Å line indicated a population inversion of levels 3 and 4 relative to level 2, hence the 182 Å and 135 Å lines are not affected by optical trapping. In the transverse direction, the intensities of both lines are mainly due to spontaneous emission because of the small plasma thickness. In the axial direction, some small enhancement of line CVI 135 Å is expected from theoretical calculations (in the order of E ≈ 1.5-2.0) and

can be taken into account (with only small corrections in the gain) by the second method.

In the second method, the intensity of a given line in the axial direction relative to the same line in the transverse direction (after adjustment for the distribution of the CVI 182 Å line intensity along the column and its approximate radial profile) was compared using the relative intensity calibration data from the spark and vertical fiber plasmas.

$$E = \frac{I(182)_{axial} \times \ell_{eff}^{-1}}{I(182)_{transv.} \times d_{eff}^{-1}} \qquad (2)$$

where ℓ_{eff} and d_{eff} are effective length and width of the plasma where CVI effectively radiate.

The enhancement, E, is related to one-pass gain, G, averaged over line profile by

$$E = (\exp G - 1)/G \; . \qquad (3)$$

where $G = k\ell$.

5.0 EXPERIMENTAL RESULTS

The improvement in focusing of the CO_2 laser resulted in a significant increase of the CVI 182 Å line axial intensity in comparison with the CVI 33.7 Å line using the same target (carbon disc with a 1 mm hole) and with a solenoidal magnetic field of 50 kGauss. Under these conditions, the intensity ratios of the CVI 182 Å to 33.7 Å lines, as well as the 182 Å to neighboring lines; in particular, the OVI 173 Å line, increased by a factor of 2 to 3 in comparison to our earlier data.

The CVI 182 Å line was observed in time integrated spectra and in time resolved measurements with enhancement (E) of up to 10, corresponding to a gain length product of $G = k\ell \approx 3.5$. In those experiments, a carbon disc with a 1.5 mm hole in the center was used. Gain was measured along the axis of the plasma column (the axis of the column was close to the center of the hole). However, radial profiles of the CVI line radiations measured with the transverse XUV duochromator by a shot-to-shot vertical scan indicated that much better conditions for maximum gain should exist in the off-axis region of the plasma column in agreement with theoretical expectations. In the center of the plasma column, the temperature is at a maximum and decreases rapidly in the outer region, whereas electron density reaches a maximum off-axis. In this way, C^{6+} ions are created mainly in the center of the plasma column and recombine (creating CVI) in the outer region where n_e is at a maximum and T_e is significantly lower than on the axis. The carbon disc target was masked to enable the axial and transverse spectrometers to observe only the off axis region of the plasma.

In order to find the radial region of the plasma column with the maximum one-pass gain, G, the CO_2 laser was focused on the target (Fig. 3b) at different radial positions. Figure 4 shows the results of such measurements for B = 90 kG and laser energy $P_{CO_2} \approx 450$ J. One may see that for this laser energy the enhancement rises rapidly near r ≈ 1.5 mm (Fig. 4 suggests that a higher resolution scan may reveal the maximum gain to be near r ≈ 2 mm). For a lower laser energy, $P_{CO_2} \approx 300$ J, which we found to be optimum in experiments with the C-disc, the maximum enhancement was observed in a relatively thin cylindrical shell of radius r ≈ 1.3-1.5 mm with enhancement close to 10 near r = 0 in agreement with our earlier results.

5.1 THE EFFECT OF MEDIUM Z ELEMENTS ON ENHANCING LOSSES BY RADIATION COOLING

During the year, the effectiveness of medium Z elements, particularly aluminum, in cooling a transient high density plasma by radiation losses was investigated both through computer simulations and experimentally. A coupled set of rate equations for either carbon, or carbon with aluminum, was solved in time self consistently with a set of energy equations which described the electron temperature. The peak value of the laser power was chosen to yield the same peak electron temperature for both cases. Figure 5 shows that the effectiveness of the radiation cooling was about 2.8 times greater for the carbon and aluminum system than for the case with carbon alone. In both instances the total number of ions was 4.5×10^{17} cm^{-3} and the electron density was approximately $\sim 6 \times 10^{18}$ cm^{-3}.

Figure 5 also indicates that aluminum plays a significant role in the process of faster radiation cooling for electron temperatures, T_e, below 100 eV. Aluminum is especially important for plasma cooling below 20-30 eV. Experimentally we observed higher CVI 182 Å line intensity in the spectra and a faster decay time of the CVI line intensities with Aℓ than without. However, enhancement of the CVI 182 Å line intensity of the aluminum coated target did not differ substantially from the plain carbon disc target. One possible explanation may be an improper concentration of Aℓ in the carbon plasma.

5.2 ENHANCEMENT MEASUREMENTS FOR CARBON FIBERS WITH AND WITHOUT ALUMINUM COATINGS

Some initial studies were conducted with carbon fibers suspended along the axis of the CO_2 laser beam. A typical experimental setup, in which the carbon fibers were supported by spider web strands of approximately 1 μ, or by

13 μ diameter carbon strands is shown in Fig. 6. The diameter of the fibers varied from 20 microns to 300 microns and the length from 2 mm to 10 mm. These fibers were thicker than those used in a similar experiment at Hull University, based on the premise that thicker fibers would enhance the plasma cooling due to fast heat transport to the fiber, for which only the thin layer was charged to the plasma. This results in rapid cooling by neutral carbon influx and thermal conduction to the cold fiber core. The measured enhancement obtained with a 75 micron by 4 mm fiber for 182 Å radiation was about 5.3, corresponding to a $k \cdot \ell \approx 3.0$ (Fig. 7). A similar experiment using 20 μ x 10.7 mm fibers, without aluminum coating, in a 90 kG magnetic field also yielded a gain $k \cdot \ell \approx 3.0$. (See Fig. 8.) Higher enhancement of $E \approx 7.1$ was obtained for a 4 mm long C-fiber coated with 8000 Å Aℓ. This corresponds with gain/length $\approx 7.5\ cm^{-1}$.

5.3 MEASUREMENTS OF ENHANCEMENT (~ 100) FOR CARBON DISC TARGETS WITH AND WITHOUT CARBON BLADES

In Fig. 9 are shown intensities of 182 Å and 135 Å lines (first and second column, respectively) measured in axial and transverse directions for a C-disc without blades. The intensity of the CVI 33.7 Å line was similar for both shots. The energy of the CO_2 laser was $P_{CO_2} \approx 300$ J, and magnetic field B = 90 kG. The CO_2 laser was focused at r = 1.3 mm from the edge of the slot (maximum enhancement region). The maximum enhancement E ≈ 100 was measured from intensity ratios of the 182 Å and 135 Å lines in the axial and transverse directions (first method) at the time of peak intensity of the 182 Å line. The one-pass gain G ≈ 6.5 was deduced from Eq. (1).

In experiments with a thin, 2 cm long C-blade attached to the disc (Fig. 3b), the intensities of the 182 Å and 135 Å lines increased typically by

a factor of 4 in the axial direction. However, the enhancement (gain) of the 182 Å line did not increase. The enhancement E ≈ 95 for the CVI 182 Å line (corresponding to a gain of G ≈ 6.5) was measured by the first method. The intensity of the CVI 33.7 Å line was well reproducible for both laser shots. Due to the increased intensity of the 135 Å line, the effect of background radiation was much smaller than in Fig. 9. The transverse instrument viewed 5 mm of plasma length (the region 1-6 mm from the disc surface), where the intensity of the CVI lines was strongest. Measurement of the CVI line intensities at different distances from the C-disc (using a 1 mm wide vertical mask) revealed that the effective length of the plasma where the density of the CVI ions was sufficiently large and uniform, was $\ell_{eff} \approx 1$ cm, although the plasma column observed by a streak camera (in visible light, i.e., in light from ions of lower stage of ionization) was significantly longer.

For the data presented in Fig. 10, the enhancement, measured by the second method, was E ≈ 120, about 25% higher than measured by the first method. This small difference is due to the enhancement E ≈ 1.3 (G ≈ 0.5) of the CVI 135 Å line (measured by the second method). Such a small enhancement for the 135 Å line in comparison with the enhancement for the 182 Å line is in agreement with theoretical predictions. Two additional checks of the enhancement measurement were made. First, the relative population of level n = 3 of the CVI ion, measured from the 182 Å line emission in the transverse direction was in good agreement with such a population obtained from the 182 Å line spontaneous emission (intensity ∝ E) in the axial direction. Second, the black-body temperature $T_B \approx 1.2$ keV obtained from the 182 Å line axial brightness $I \approx 10^5$ W/sr (Fig. 10), based on a source area of 8×10^{-4} cm^2 was much higher than the temperature of the recombining plasma ($T_e \approx 10$-20 eV) which was emitting this radiation. The black-body temperature was estimated from Raleigh-Jeans formula assuming a Doppler broadened 182 Å line width $\Delta\lambda_D \approx 10^{-2}$ Å.

5.4 POPULATION INVERSION IN NeVIII

Work continued on the population inversions in the lithium (Li) like series CIV, OVI, FVII and NeVIII, with results being observed with time resolution instrumentation. Neon gas was puffed into the target chamber, and was localized to a region 5 cm long by mechanical apertures. Initial gas pressure was controlled by varying the relative timing of the laser pulse with respect to the gas valve opening. The populations of the 4d and 3d levels were obtained from the measurements of the NeVIII 73.5 Å (4d - 2d) and the NeVIII 98.2 Å (3d - 2p) transitions in the transverse direction using the XUV duochromator. The column density populations were determined from the absolute intensity. Because these two lines are close together, the variation in sensitivity of the instrument is small and was neglected. Hence, the relative population of the 4d and 3d levels can be more accurately determined than the absolute populations. Population levels of the 4d and 3d levels of NeVIII as a function of initial gas pressure are shown in Fig. 11. It can be seen that the 4d population exceeds the 3d population level in the range of gas pressures from 12-15 torr. Since the 4d and 4f levels are expected to be closely coupled by collisions, this leads to gain on the 4f - 3d transition at 292 Å. The effect of optical trapping in the radial direction on the observed 73 Å/98 Å ratio was checked by measuring the ratio of the intensity of the fine structure components of the 98 Å line by the XUV duochromator. This was close to the theoretical value for an optically thin plasma. The NeVIII 292 Å line was also observed in the axial direction, but we did not observe a significant increase at high neon pressures, possibly due to absorption in the neutral gas boundary. Further development of the gas puffing technique should alleviate this problem.

6.0 CONCLUSION

In FY 1984, we measured an enhancement of stimulated emission over spontaneous emission larger than E ≈ 100 (one-pass gain G ≈ 6.5) for the CVI 182 Å line in a magnetically confined, recombining plasma column. This enhancement (averaged over the spectral line profile) was measured at a distance r ≈ 1.3-1.5 mm from the column axis by two independent techniques. A black-body temperature T_B ≈ 1.2 keV was calculated from the 182 Å line intensity in the axial direction (I ≈ 10^5 W/sr) and exceeds by a factor 60-120 the plasma temperature in the recombination stage. Various target configurations were evaluated, and the effect of medium Z elements on radiation cooling was also investigated. Also, maximum population inversion of the 4d and 3d levels of NeVIII as a function of initial gas pressure was determined by experimental results.

7.0 FIGURE CAPTIONS

Fig. 1 Schematic of Experimental Arrangement.

Fig. 2 Target Assemblies

a) Gas target;

b) Carbon blade;

c) Carbon fiber;

d) Carbon disc with four aluminum blades.

Fig. 3a Carbon disc with mask but without carbon blade.

Fig. 3b Carbon disc with mask and with carbon blade.

Fig. 4 Graph of enhancement of 182 Å line vs. distance from slot for carbon disc target with carbon blade.

Fig. 5 Computer calculation of effectiveness of radiation cooling for carbon and carbon-aluminum plasmas.

Fig. 6 Detail of carbon fiber target.

Fig. 7 Axial and transverse CVI 182.17 Å (3-2) time evolved line intensities for a 4 mm x 75 μ dia graphite fiber target yielding a gain $k\ell \approx 3.0$.

Fig. 8 Axial and transverse CVI 182 Å time evolved line intensities for a 10.7 mm x 20 μ dia carbon fiber target in a 90 kGauss field yielding a gain $k\ell \approx 3.0$.

Fig. 9 Time evolution of CVI 182 Å and 135 Å line intensities measured with axial and transverse XUV instruments for two discharges with the same plasma conditions. The enhancement of stimulated emission for the 182 Å line was $E \approx 100$ (one-pass gain $k \times \ell \approx 6.5$).

Target: carbon disc with horizontal slot.

Laser: 1.3 mm from slot.

Fig. 10 As in Fig. 3, but with a thin carbon blade attached to carbon disc. The enhancement was $E \approx 95$ ($k \times \ell \approx 6.5$).
Note four times higher intensities than for C-disc without C-blade.

Fig. 11 Population inversion of the 4d and 3d levels of NeVIII as a function of initial neon pressure.

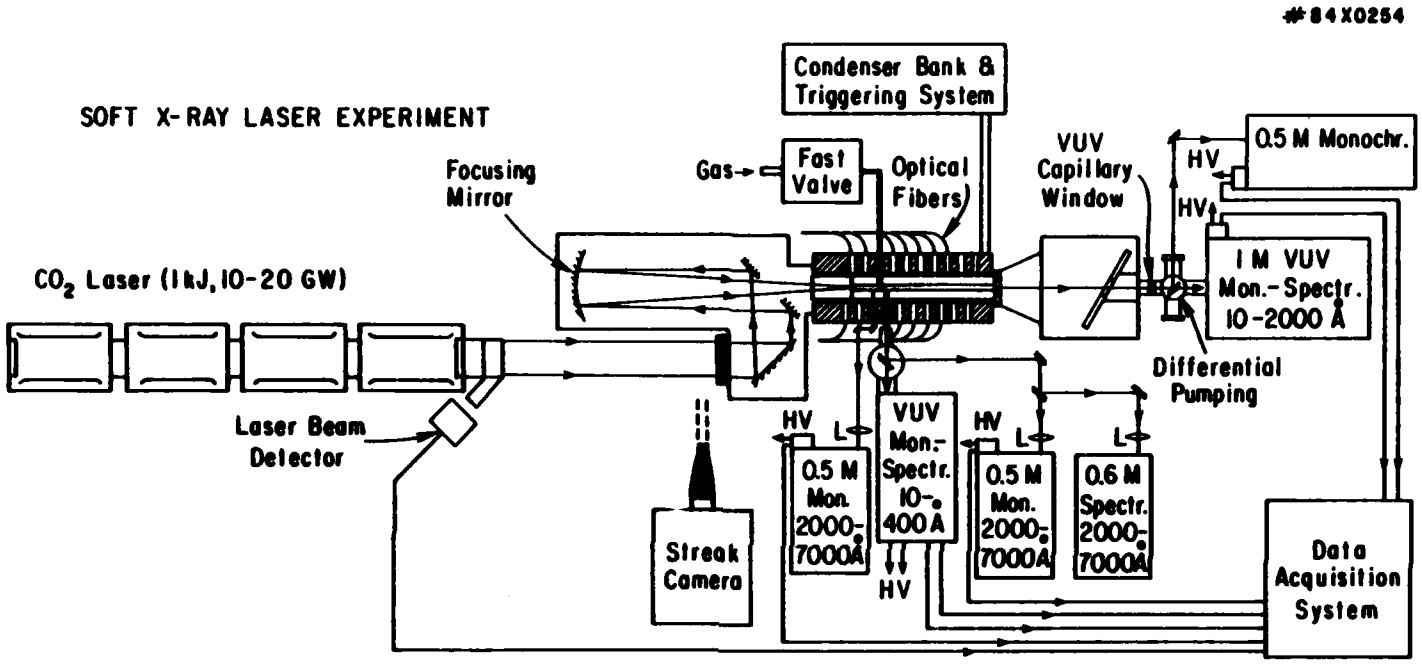
#84X0254
SOFT X-RAY LASER EXPERIMENT
Condenser Bank & Triggering System
Focusing Mirror
Gas
Fast Valve
Optical Fibers
VUV Capillary Window
HV
0.5 M Monochr.
HV
CO_2 Laser (1kJ, 10-20 GW)
1 M VUV Mon.-Spectr. 10-2000 Å
Differential Pumping
Laser Beam Detector
HV
L
VUV Mon.-Spectr. 10-400 Å
HV
L
L
0.5 M Mon. 2000-7000Å
0.5 M Mon. 2000-7000Å
0.6 M Spectr. 2000-7000Å
HV
Streak Camera
Data Acquisition System

Fig. 1

TARGET ASSEMBLIES

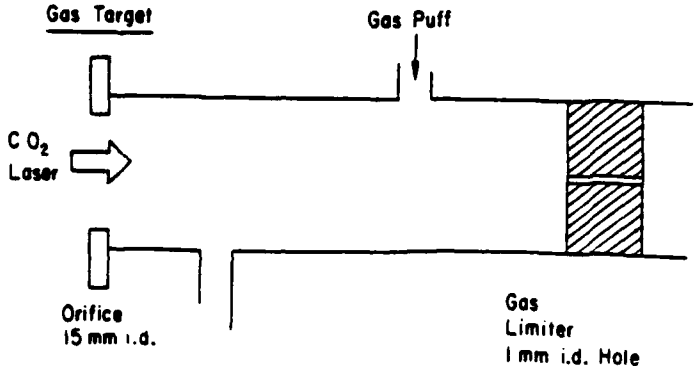

a) Gas Target

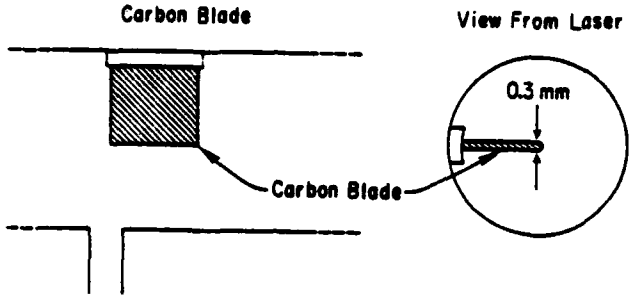

b) Carbon Blade Target

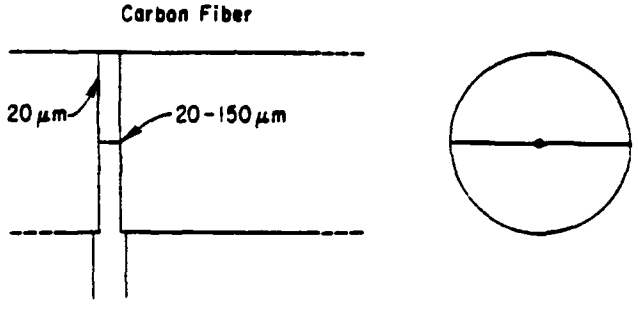

c) Carbon Fiber Target

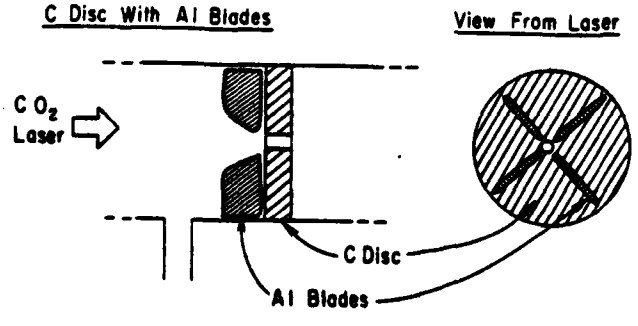

d) Carbon-disc Target With Four Al-blades

Fig. 2

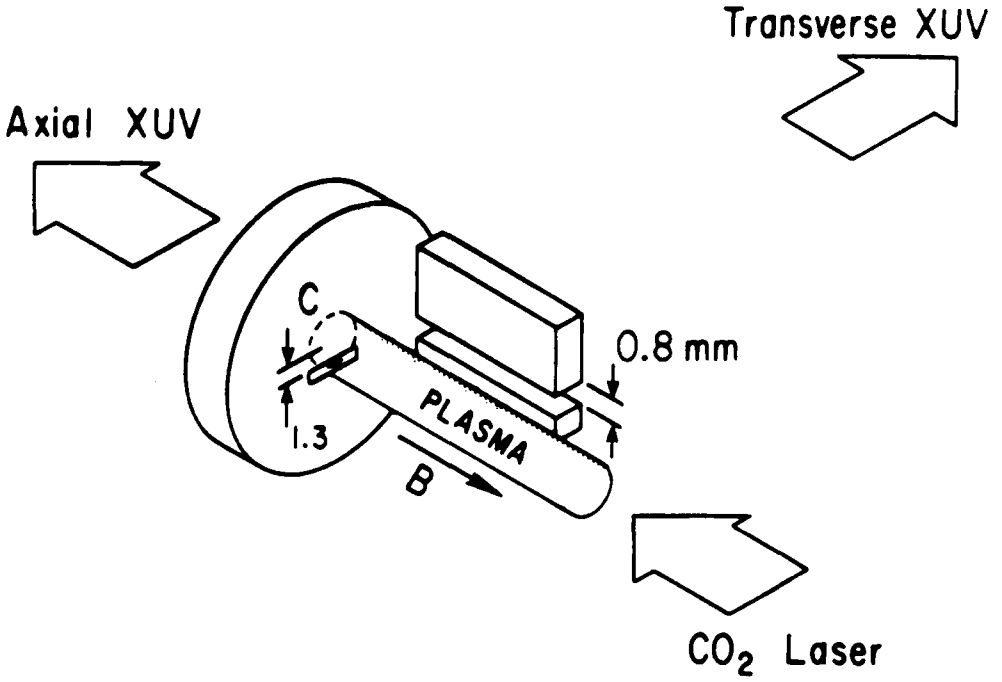
Transverse XUV
Axial XUV
C
0.8 mm
1.3
PLASMA
B
CO_2 Laser

Fig. 3a

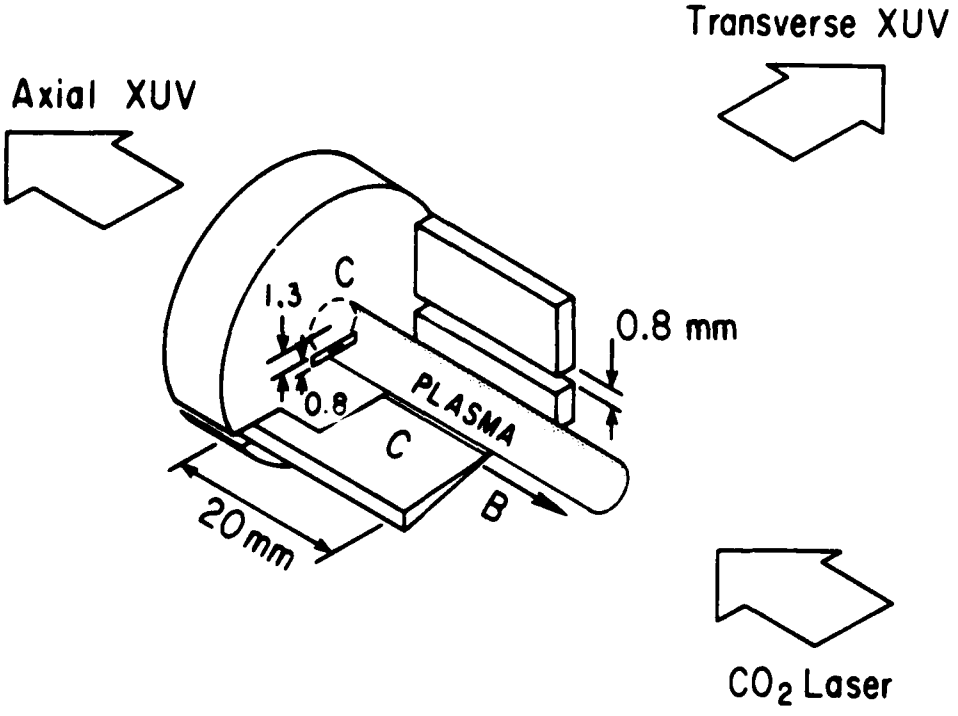
Transverse XUV
Axial XUV
1.3
C
0.8 mm
0.8
PLASMA
C
20 mm
B
CO_2 Laser

Fig. 3b

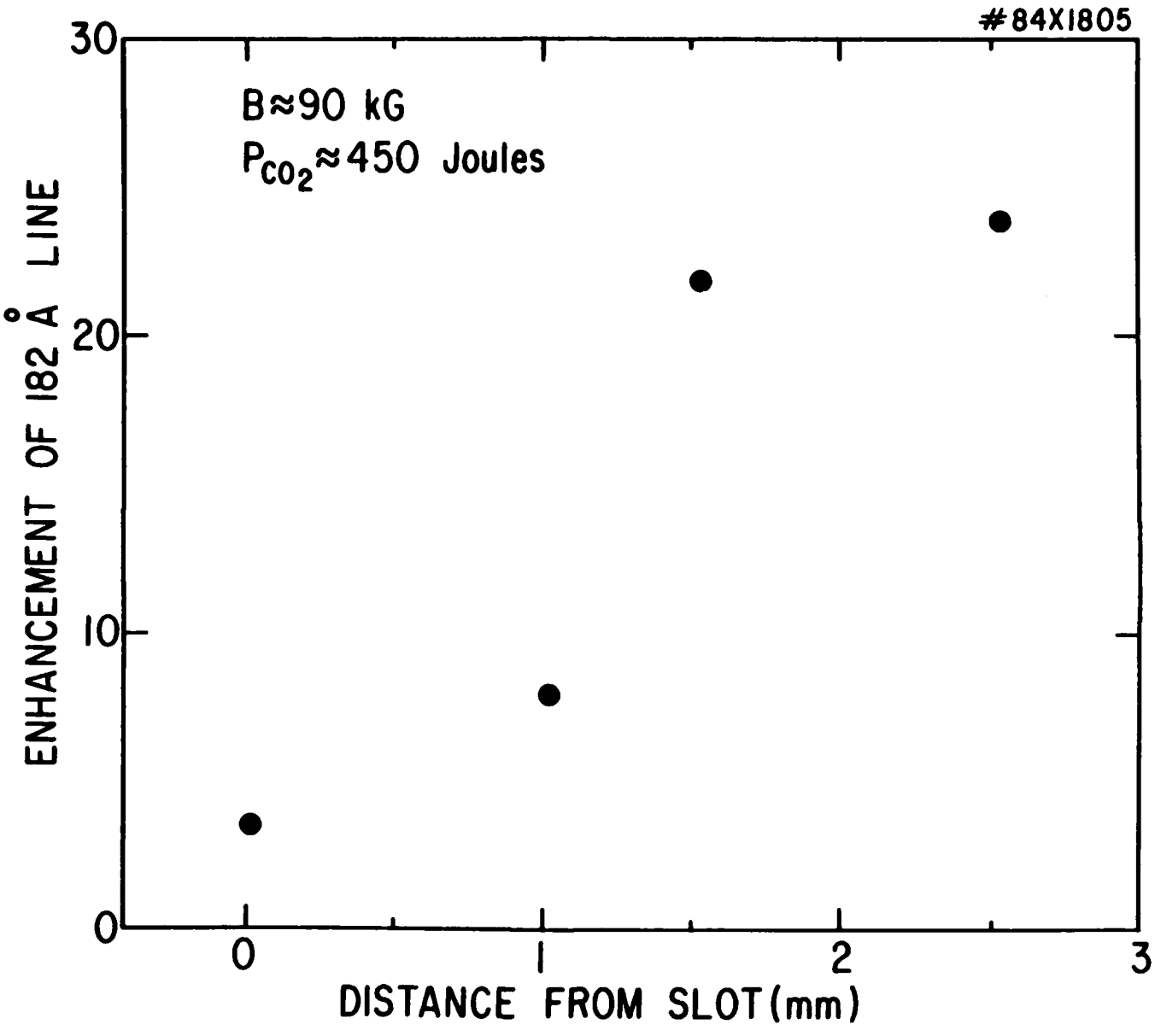
#84X1805
B≈90 kG
P_{CO_2}≈450 Joules
ENHANCEMENT OF 182 Å LINE
30
20
10
0
0
1
2
3
DISTANCE FROM SLOT(mm)

Fig. 4

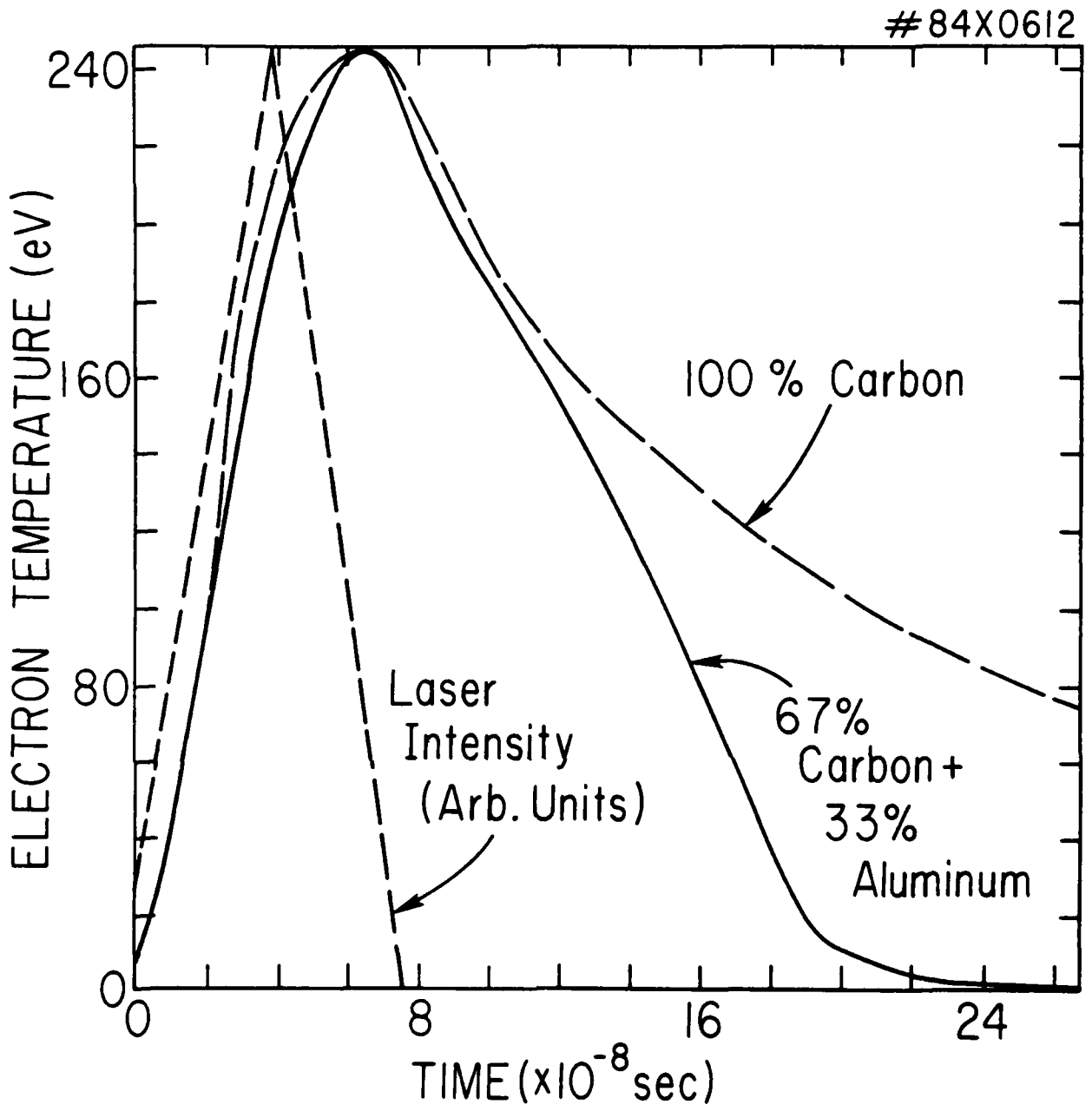
#84X0612
240
160
80
0
ELECTRON TEMPERATURE (eV)
100 % Carbon
Laser
Intensity
(Arb. Units)
67%
Carbon +
33%
Aluminum
0
8
16
24
TIME (x10^-8 sec)

Fig. 5

#84X1502

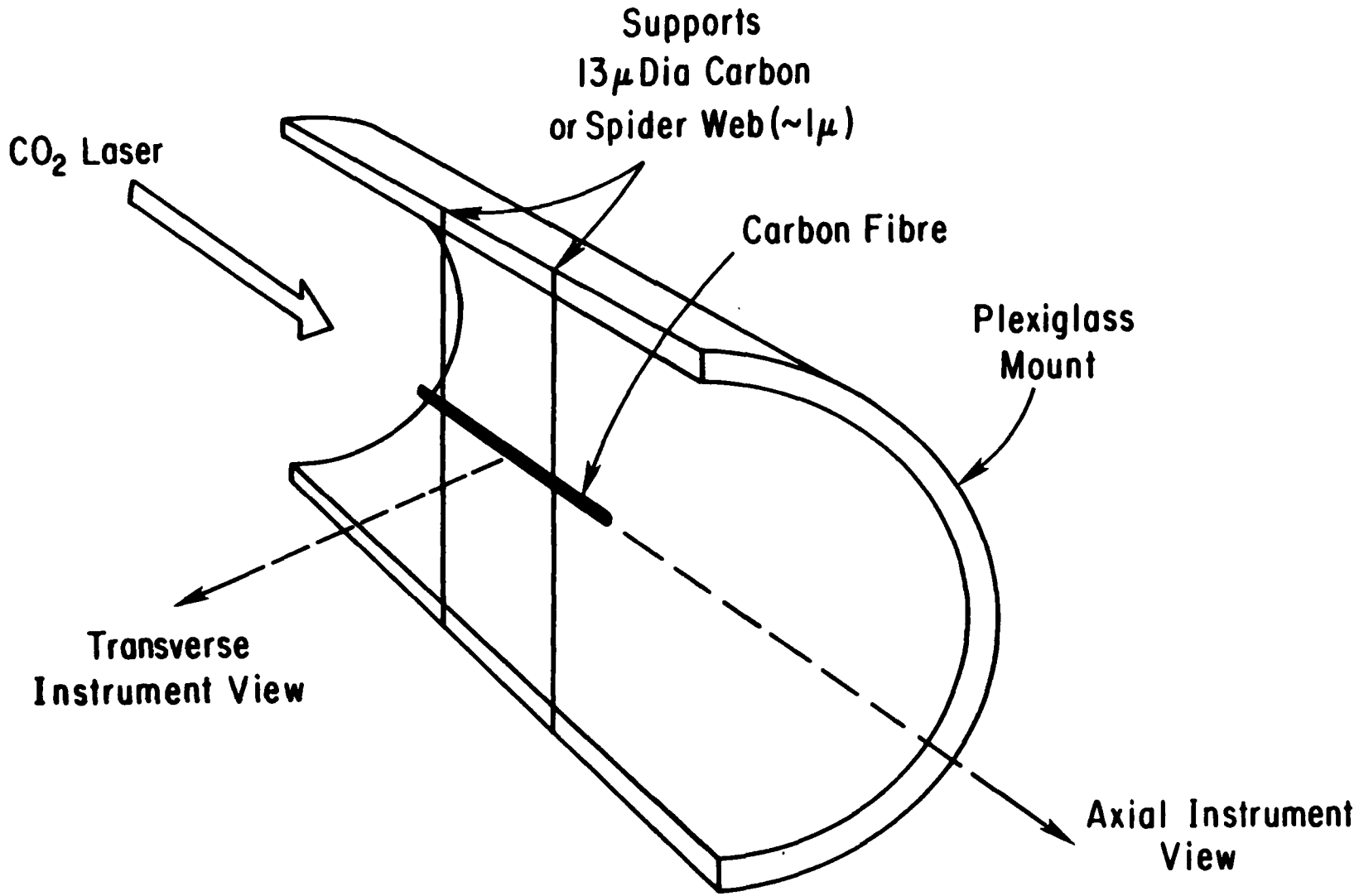

Fig. 6

GRAPHITE FIBRE TARGET

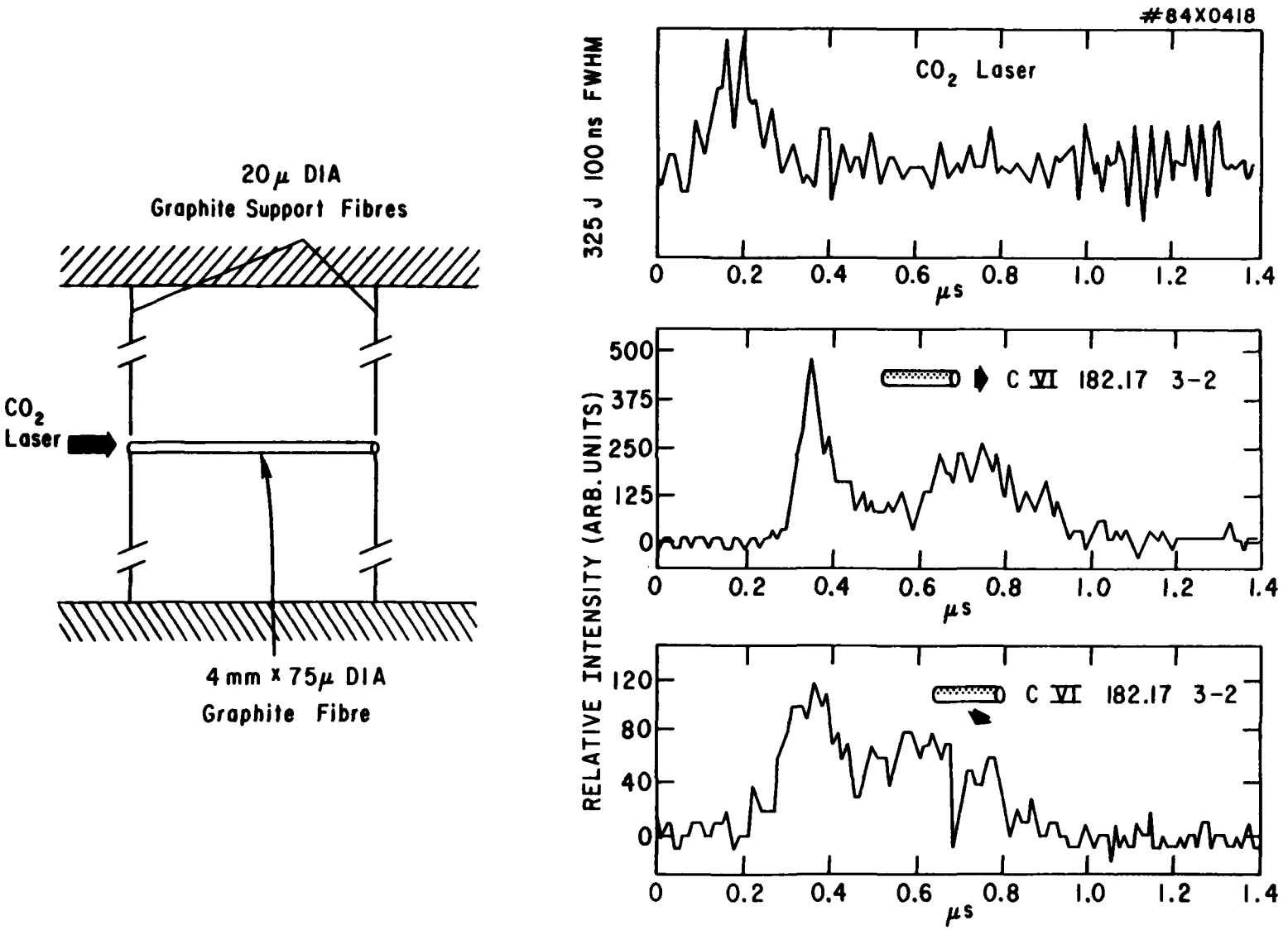

Fig. 7

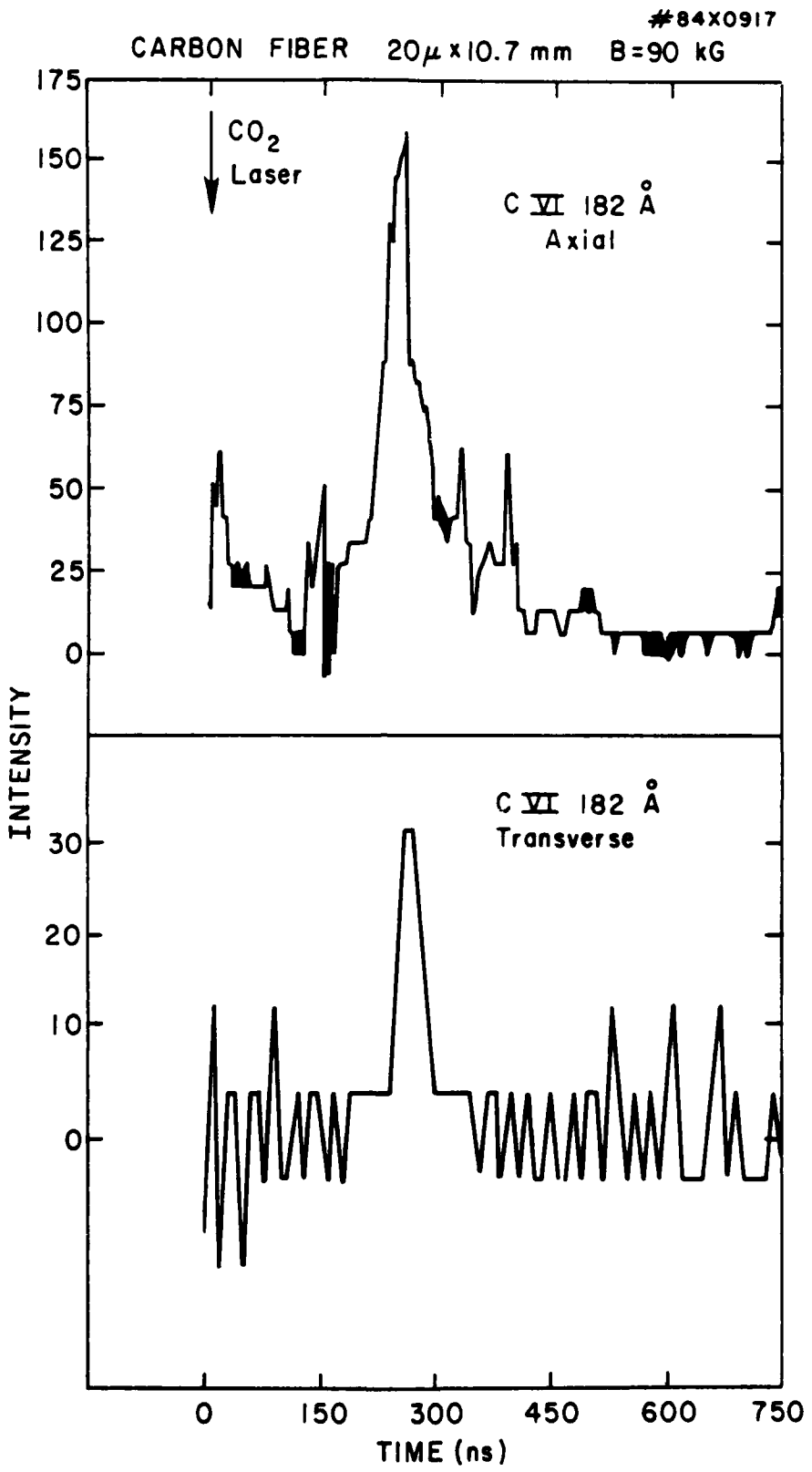
#84X0917
CARBON FIBER 20μ x 10.7 mm B=90 kG
CO2 Laser
C VI 182 Å
Axial
C VI 182 Å
Transverse
INTENSITY
175
150
125
100
75
50
25
0
30
20
10
0
0
150
300
450
600
750
TIME (ns)

Fig. 8

#85X0182

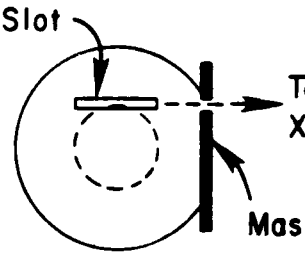

B = 90 kG

$P_{CO_2} \approx 300$ J

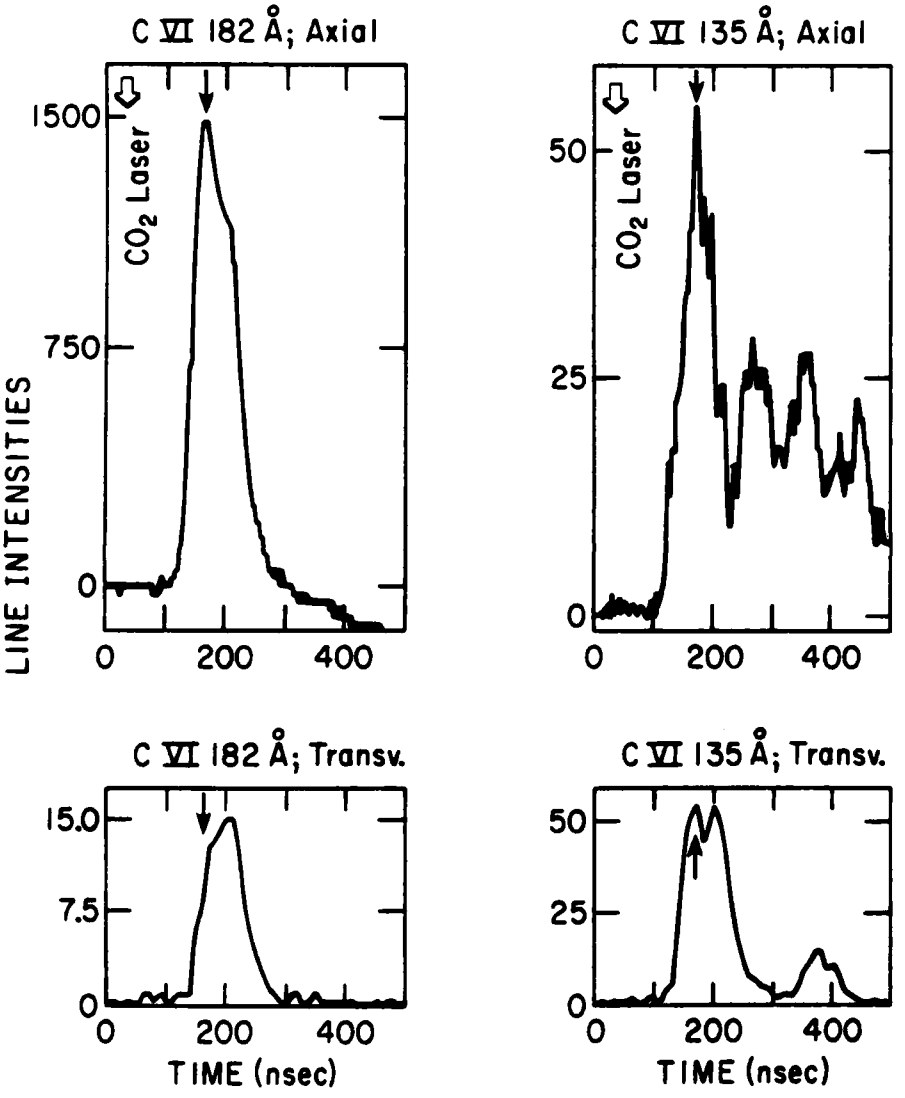

$$E = \frac{I(182)_{axial}}{I(182)_{transv.}} \Big/ \frac{I(135)_{axial}}{I(135)_{transv.}} \approx 100$$

#1967 #1966 Oct. 9/84

Fig. 9

#85X0184

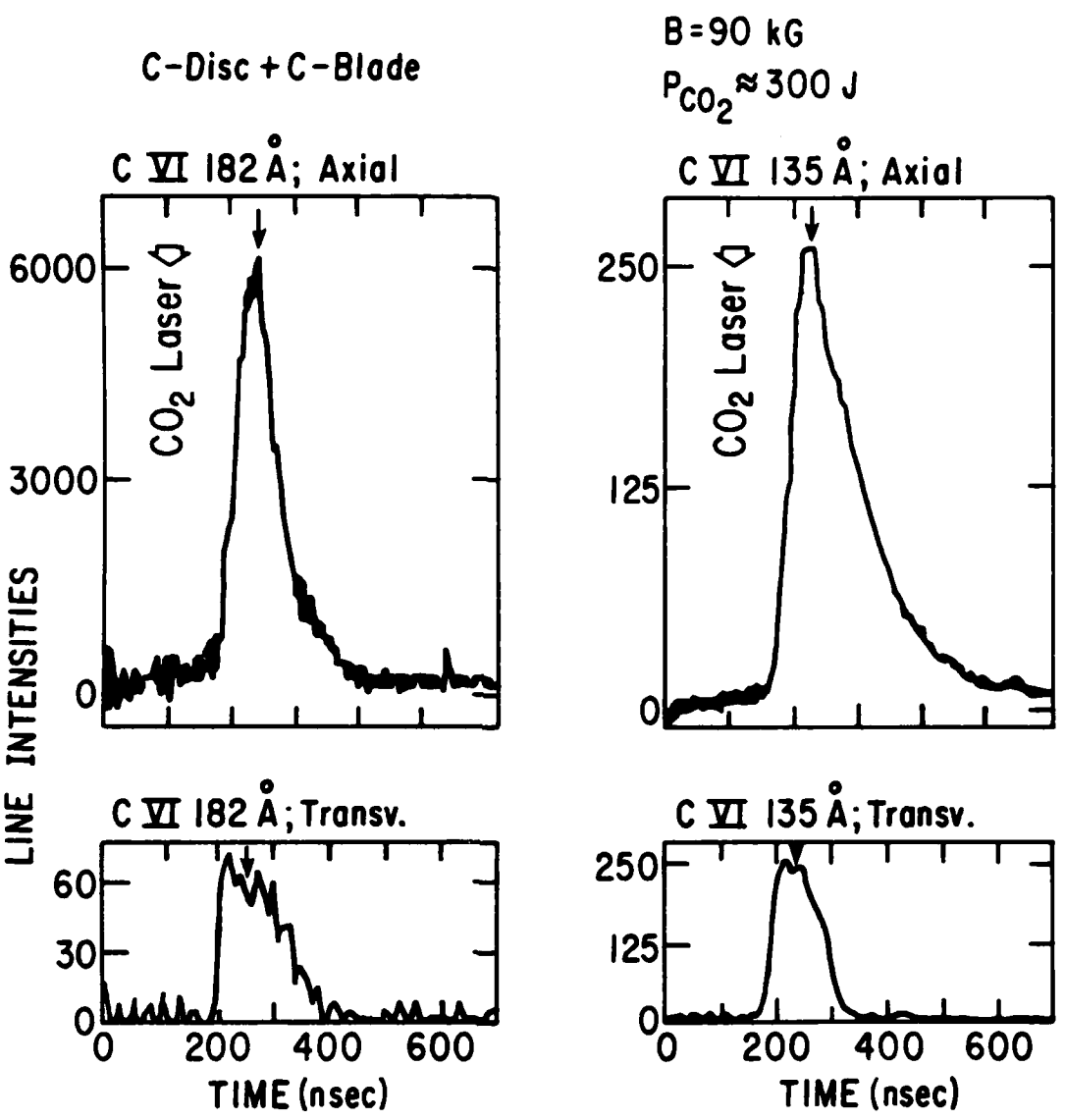

$$E = \frac{I(182)_{axial}}{I(182)_{transv.}} \Big/ \frac{I(135)_{axial}}{I(135)_{transv.}} \approx 95$$

#2237

2245 Oct.23,84

Fig. 10

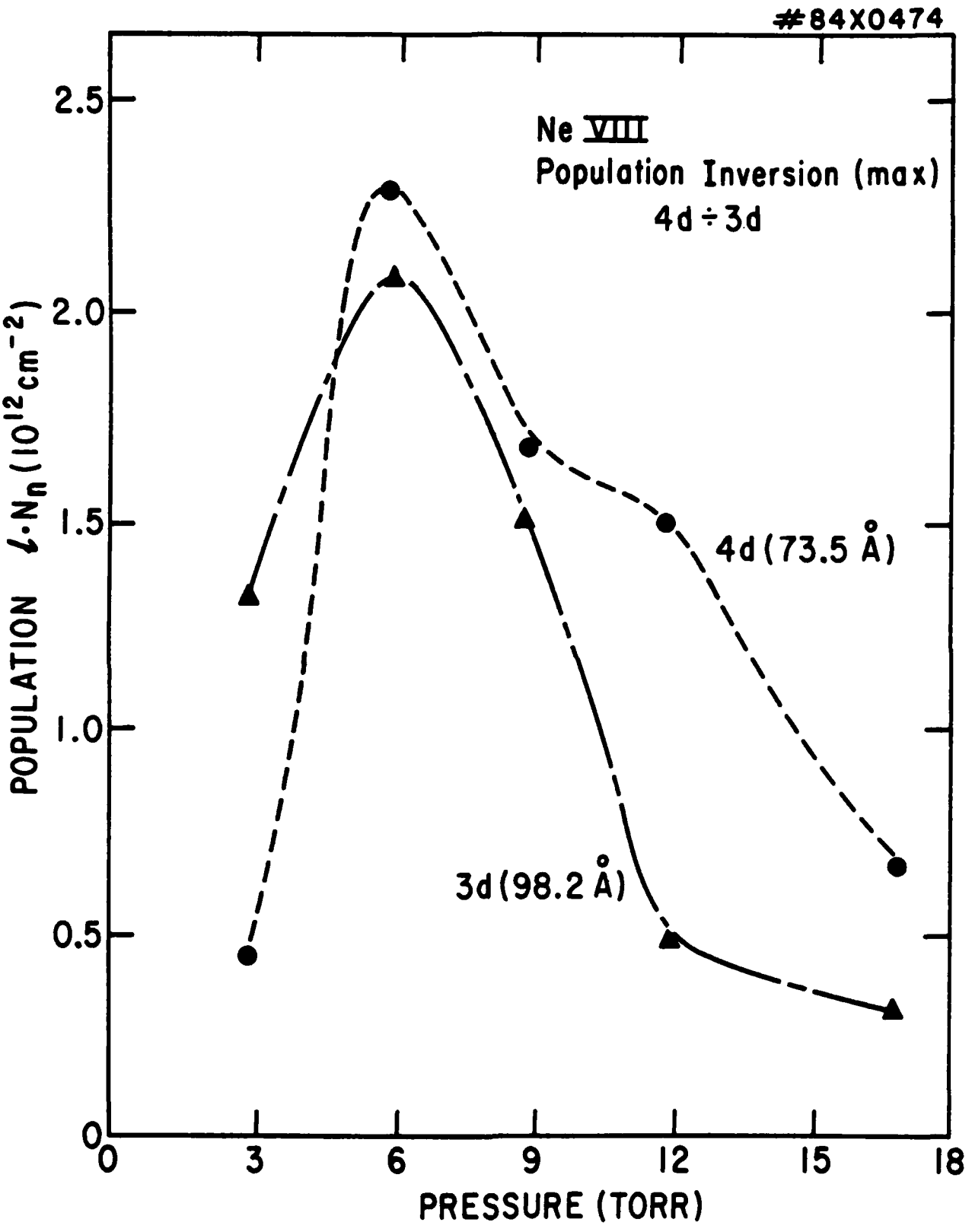
#84X0474
Ne VIII
Population Inversion (max)
4d ÷ 3d
4d (73.5 Å)
3d (98.2 Å)
POPULATION $\ell \cdot N_n$ (10^{12} cm^{-2})
PRESSURE (TORR)
0
0.5
1.0
1.5
2.0
2.5
3
6
9
12
15
18

Fig. 11

END

FILMED

11-85

DTIC